2024 IEEE International Conference on Robotics and Automation (ICRA 2024)
May 13-17, 2024. Yokohama, Japan

Magnetic Mobile Micro-Gripping MicroRobots (MMμGRs) with Two Independent Magnetic Actuation Modes

Aaron C. Davis[1], Emmett Z. Freeman[1] and David J. Cappelleri[1,2]

***Abstract*— In this paper, we introduce magnetic mobile micro-gripping microrobots with two independent actuation modes. By aligning two magnets with slight variations in magnetic moment orientations, we create a net magnetic moment for precise position and orientation control through external fields, while harnessing opposing torques on the magnets to induce internal stresses needed for gripping. Our microrobot design features a compliant spring-like structure for significant deflection, enabling a gripping motion under specific magnetic field conditions. Magnet rotation allows precise control over gripper actions, returning to a default state (normally open or closed) when the magnetic field diminishes. This work advances magnetic field-controlled microrobotics, bridging the millimeter-to-micrometer gap. It holds promise for applications in microsurgery, micro-assembly, and microscale exploration.**

I. INTRODUCTION

Microrobotics has emerged as a dynamic field, offering innovative solutions for tasks at the microscale that were once deemed unattainable. With applications spanning various domains, including medicine, manufacturing, and scientific research, the quest to create agile and precise microrobots has ignited a fervent pursuit of novel control mechanisms and design strategies.

The utilization of magnetic fields as a means of controlling microrobots has garnered substantial attention in recent years [1]. Researchers have successfully harnessed magnetic actuation, leveraging its non-invasive nature and high precision to navigate the complex and constrained environments encountered at the microscale [2], [3]. This approach has enabled remarkable achievements, particularly in the realm of biomedical applications [4]. Beyond propulsion, magnetic fields have also been employed to manipulate the morphology of microrobots [2], [5]–[7]. The integration of compliance and flexibility into microrobot designs has been a key focus. Compliant structures have been instrumental in enhancing microrobot adaptability [8], [9]. These structures enable deflection and gripping actions, expanding the microrobot's utility. These advancements collectively underscore the profound impact of magnetic field-based microrobotics and micromanipulation techniques. This article seeks to contribute to this exciting landscape by presenting an innovative approach to magnetic field-controlled microrobots, building upon the rich foundation laid by prior research.

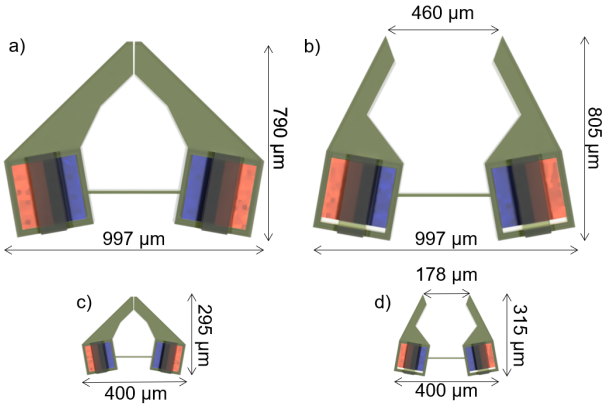

Fig. 1: Magnetic Mobile Micro-Gripping microRobots (MMμGRs) with two independent magnetic actuation modes. When in the presence of a magnetic field, the relative alignment of embedded permanent magnets allows for magnetic torques to be generated for opening/closing of the grippers. Additionally, magnetic gradients are used for locomotion and orientation control. The schematic shows normally closed and normally open versions of MMμGR-L and MMμGR-S designs.

While magnetic propulsion has become one of the most popular techniques for utethered microgrippers, magnetic actuation has primarily been used on robots in the mesoscale [9]–[11]. Smaller robots rely on thermal, optical, and chemical methods of actuation [12]–[15]. We present the design, characterization, and testing of Magnetic Mobile Micro-Gripping microRobots (MMμGRs) with independent magnetically-driven locomotion and actuation modes (Fig. 1), producing the smallest micro-gripper to be actuated and controlled exclusively using magnetic fields. Through a comprehensive exploration of design, fabrication, and computer model and experimental validation, this work aims to further expand the horizons of microrobotics and micromanipulation, promising new dimensions of control and functionality in microrobotic systems.

II. DESIGN

A. Design Overview

Leveraging the design flexibility of 3D printing technology, we engineered the MMμGRs with dual cube magnets to harness the internal torques generated by the presence of multiple magnetic domains aligned in varying directions. (Fig. 2). The magnetic force, $\vec{F}_m$, and torque, $\vec{T}_m$, on a magnet with magnetic moment, $\vec{m}_r$, in an applied field, $\vec{B}$

*This work was supported by the National Science Foundation under NSF IIS Award #: 1763689 and NSF CMMI Award #: 2018570 and the National Institute of Health under NIH Award #: 1U01TR004239-01

[1]Aaron C. Davis, Emmett Z. Freeman, and David J. Cappelleri are with the School of Mechanical Engineering, Purdue University, West Lafayette, IN 47907, USA. {davi1381,freem129,dcappell}@purdue.edu

[2]David J. Cappelleri is also with the Weldon School of Biomedical Engineering (By Courtesy), Purdue University, West Lafayette, IN 47907, USA.

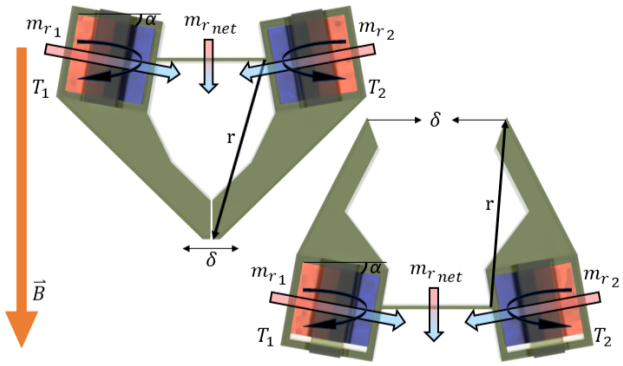

Fig. 2: Free body diagrams illustrating the magneto-mechanical interactions within the normally closed (left) and normally open (right) configurations. The presence of magnetic field $\vec{B}$, in the direction of $m_{r_{net}}$, produces the required magnetic torque to open or close the gripping jaws.

are:

$$\vec{F}_m = (\vec{m_r} \cdot \nabla)\vec{B}$$

$$\vec{T}_m = \vec{m_r} \times \vec{B}$$

When two or more magnets are put together in a body, or in this case a microrobot, the net magnetic moment, $m_{r_{net}}$, will be the sum of the magnetic moments. When a field is applied, the microrobot experiences a net torque, which rotates the microrobot to align with the field, and a net force which pulls the microrobot along the field's gradient. When the net magnetic moment of the microrobot is aligned with the applied field it experiences zero net torque. However, if the magnetic moments of the individual magnets are not all aligned with each other, they will continue to experience localized torques. This effect can be utilized to create an actuating mechanism. Here, we have used this principle to design both normally open (NO) and normally closed (NC) MMµGR variants (Fig. 2), which also have an independent locomotion modes through the use of magnetic field gradients.

The torque generated is dependent on the magnetic moment of the magnets, which can be calculated from the volume, V, and the magnetic remanence, B_r:

$$m_r = \frac{B_r V}{\mu_0}$$

where μ_0 is the magnetic permeability of free space. Compared to magnetic micro and nano particles [10], [16], [17] or magnetic films [18], [19] often used in microrobotics, the solid N52 NdFeB permanent cube magnets (SM Magnetics) chosen for this design offer a stronger magnetic moment due to the greater volume of magnetic material.

For a two magnet microrobot, the torque exerted on each of the magnets is proportional to the sine of the magnet alignment angle α (Fig. 2). The greater the torque we can apply to the magnets, the stronger the gripping force is, but there is a trade-off. $m_{r_{net}}$ is proportional to the cosine of α which directly controls the locomotion of the microrobot. Any change in α to increase the torque decreases

TABLE I: Design dimensions for the large and small MMµGRs.

Parameter	MMµGR-L	MMµGR-S
NC Opening	5 µm	2 µm
NO Opening	460 µm	178 µm
Hinge Width (w)	12.5 µm	5 µm
Hinge Height (h)	250 µm	100 µm
Hinge Length (L)	350 µm	140 µm

the maneuverability of the microrobot. In other published work, microrobots are usually designed with one primary magnetic domain to avoid this issue [5], [11]. However, because of the strength of the permanent magnet bodies, an α of 10° creates a sufficiently large $m_{r_{net}}$ without dramatically decreasing the torque.

Two configurations of the gripper were designed in two different sizes. NC and NO designs for cube magnets with side lengths of 100 µm and 250 µm, respectively. We denote the smaller MMµGRs that have the 100 µm-sized magnets as MMµGR-S and the larger MMµGRs that have the 250 µm-sized magnets as MMµGR-L. The basic parameters for each design were the same with the dimensions being scaled to fit each magnet size. The difference between the NC and NO designs is that α is positive for the NC configuration and negative for the NO case. This causes the torques to switch direction when the robot is in stable equilibrium and bend the arms inwards rather than outwards. The large and small NO configuration were printed with an openings of 460 µm and 178 µm respectively. The large and small NC conficurations were printed with openings of 5 µm and 2 µm

The MMµGRs are designed with a flexible hinge, which allows bending for the micro-gripper to open, and provides a restoring force. The hinge dimensions for the design were found using the classical beam bending equations. For a beam with a length, L, greater than ten times the width, the deflection angle at the end of the hinge, θ, caused by an applied torque, T, is:

$$\theta = \frac{TL}{EI}$$

with the beam having Young's modulus, E, and second moment of area I. For a beam of height, h and width, w with a rectangular cross-section:

$$I = \frac{wh^3}{12}$$

The opening of the gripper δ is then equal to the arm length, r, multiplied by θ:

$$\delta = r\theta$$

Hinge dimensions, w, h, and L, were then chosen to satisfy the desired δ with consideration for the desired overall size and shape of the microrobot and are shown in Table I.

B. Multi-physics Model

The design of the microrobots were validated using a COMSOL Multiphysics Finite Element Analysis (FEA) model combining the magnetic and solid mechanics interactions of the system. The simple geometry of the actuating sections of the microrobot allows for a 2D model. A Young's

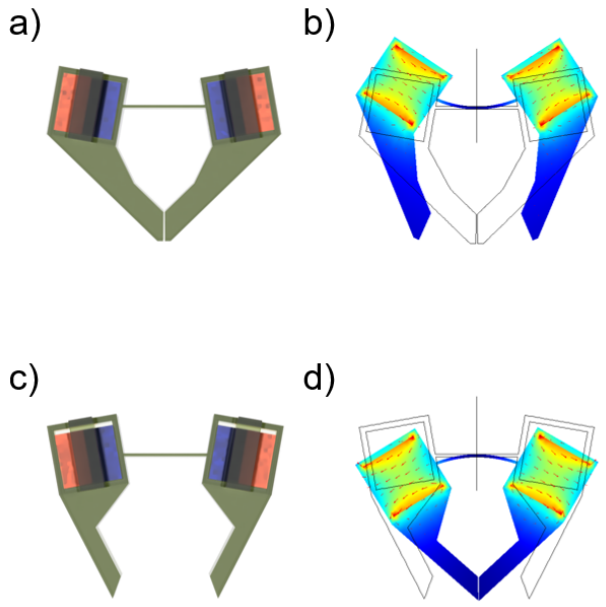

Fig. 3: Multi-physics analysis: a) Illustration of the Normally Closed (NC) microrobot design. b) The FEA model demonstrates the behavior of the NC microrobot under full actuation at 25 mT. c) Illustration of the Normally Open (NO) microrobot design. d) The FEA model showcases the behavior of the NO microrobot under full actuation at 22.5 mT. Coloration and vectors show magnetic flux density.

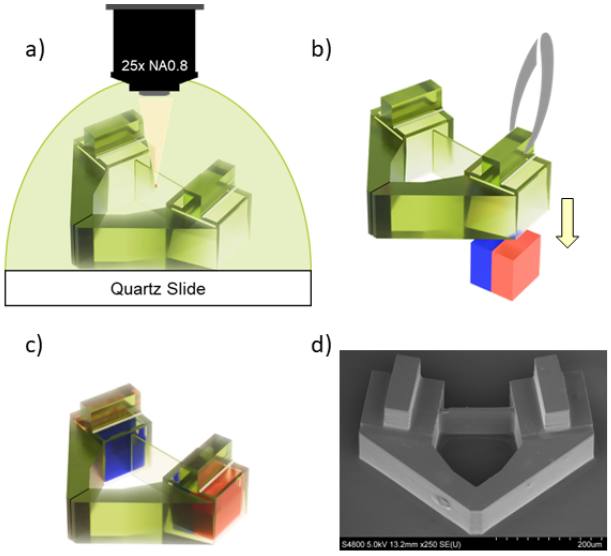

Fig. 4: MMµGRs fabrication steps. a) The body of the MMµGRs are fabricated using a two-photon 3D printer; b) The printed microrobot bodies are detached from the substrate and attached to micromagnets using superfine tweezers; c) The assembled MMµGRs are then rinsed in IPA and cured under UV light. d) A scanning electron microscope (SEM) image showcasing the detailed structure of a MMµGR-S version. Note: a 20 nm film of AuPd was sputtered on the robot to allow for imaging, which bridged the jaw opening gap of this particular normally closed design.

modulus of 2GPa for the microrobot body was retrieved from the resin manufacturer's websites. The magnetic remanence of the cube magnets was measured to be 810 mT using a DynaCool PPMS (Quantum Design) system. The results of the analysis showing the successful actuation of both the NC and NO configurations are summarized in Fig. 3. Due to the hinge stiffness and magnetic torque both scaling with L^3, the results for the MMµGR-S and MMµGR-L are identical with a scale difference of 2.5.

III. MMµGR FABRICATION

As shown in Fig. 4, the MMµGRs were fabricated out of IP-S resin on indium tin oxide coated glass substrates using a Photonoic Professional GT2 two photon 3D printer (Nanoscribe GMBH) with a 25x objective lens. The standard shell and scaffold slicing and laser settings were used. After printing, the robots were developed in SU-8 developer for 20 min. The MMµGRs were designed to have an open cavity in which the permanent magnets could sit. This cavity was printed in contact with the substrate so the resin from inside the cavity was not removed during development. This allowed the printed structures to be removed from the substrate and attached to the magnets without adding additional glue. To decrease the residual resin, sacrificial blocks were printed inside the cavities. These blocks were left behind on the glass substrate when the printed microrobot bodies were removed. In order to safely remove the microrobot bodies from the substrate, a fin was printed on the top of the magnet housing which could be gripped by fine tipped tweezers. The micromagnets were one at a time aligned on a bar magnet and the microrobot body was placed onto the micro-magnet with the cavity enclosing it. The next micro-magnet was then aligned and the microrobot body was rotated $180°$ then placed onto it. The assembled MMµGR was then carefully rinsed in IPA to remove any excess resin and then cured under a UV light for 20 min. Due to difficulties in fabrication, the 100 µm cube magnets were not coated in nickel like the 250 µm cube magnets, as is common for neodymium magnets.

IV. EXPERIMENTAL RESULTS AND DISCUSSION

A. Experimental Setup

The MFG-100-i system (Magnebotix AG), illustrated in Fig. 5, is employed to generate external magnetic fields for propelling the microrobots. This system can generate magnetic fields of up to 25mT, and gradients as high as 1.5T/m within a workspace measuring 10mm in diameter. It offers the unique capability to independently control both the orientation of the magnetic field and the direction of the gradient. Due to the relatively high stiction forces at the microscale, mobile microrobots are more effectively controlled through magnetic field gradients when they are submerged in a liquid medium. Thus, in our experimental setup, the microrobots were placed on silicon wafers enclosed by a 3D printed (FormLabs) ring and submerged in silicone oil, as depicted in the inset of Fig. 5. Since the coils in the magnetic field generating system tend to overheat if left set on a high field for an extended period of time, it is more feasible to perform micromanipulation experiments with the NC MMµGRs instead of the NO version. For this reason, most of physical characterization testing was done using the

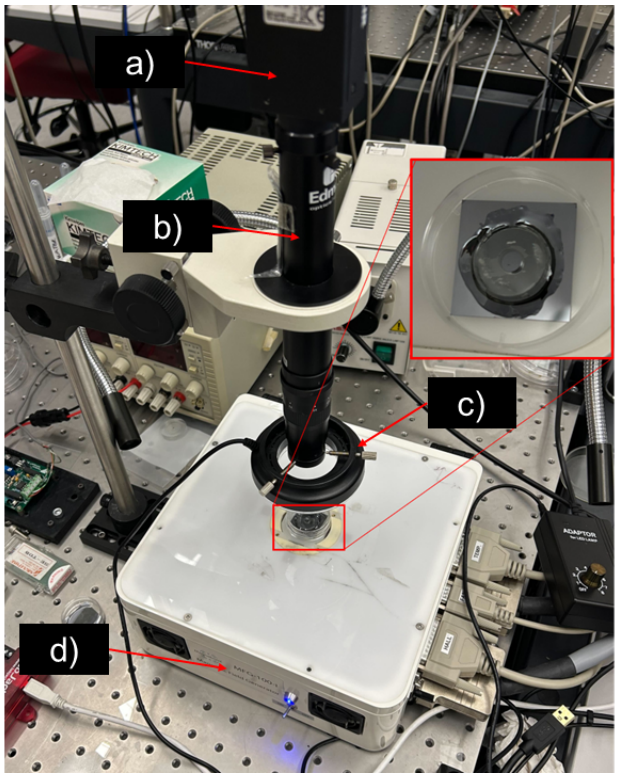

Fig. 5: Experimental setup featuring (a) CCD camera, (b) microscope, (c) light ring, and (d) the Magnetic Field Generator (MFG) system. Inset: A close-up view of the silicon substrate with silicone oil well and a MMµGR-L prototype.

NC MMµGR configuration, though the same principles apply to the NO configuration.

B. Gripper Actuation and Design Validation

Fig. 6 shows the gripping ability of the microrobots comparing their NC rest state with the active open state. The experimentally determined relationship between jaw opening and field strength (Fig. 7) can be compared to those predicted with our FEA models, providing valuable insights into the performance of our magnetic grippers. Both the physical prototypes and FEA models exhibit consistent trends, with jaw opening values demonstrating a linear response to the applied magnetic field strength. However, a notable observation is that the physical prototypes did not respond to the applied magnetic field to the extent predicted by the FEA models. This discrepancy raises important questions and considerations for our research. Several factors may contribute to the observed disparity in the grippers' response to the magnetic field.

First, the post-print curing process of the resin may have changed the mechanical properties of the physical prototypes. The curing process can introduce variations in material properties that differ from the idealized assumptions made in the FEA models. Second, the physical microrobots are inherently delicate and could possibly be damaged during the assembly process. This could potentially affect their performance and introduce discrepancies between the physical prototypes and the FEA simulations. Finally, the observed differences in

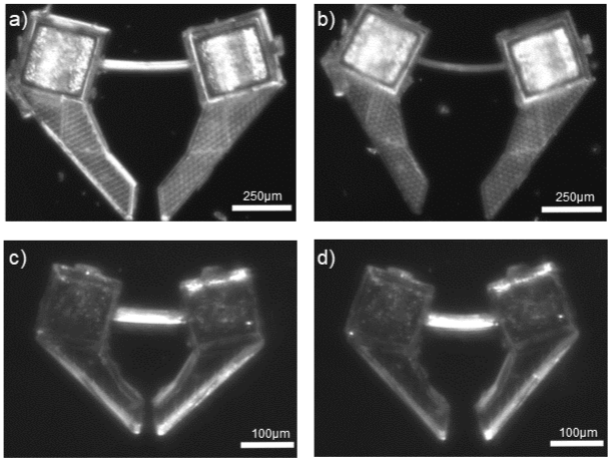

Fig. 6: Normally closed MMµGR gripping tests. A MMµGR-L version in the (a) off/closed state and (b) in the open/actuated state. A MMµGR-S version in the (c) off/closed state and (d) in the open/actuated state. The gripper openings in the off states are larger than as printed due to the interaction of the micro cube magnets.

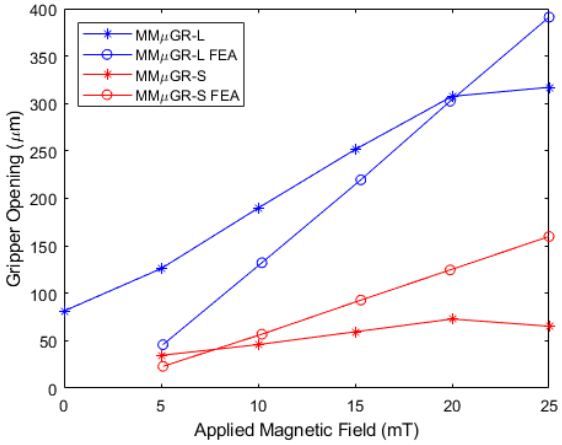

Fig. 7: Gripper jaw opening distance versus the applied magnetic field for normally closed MMµGR-S and MMµGR-L prototypes and their respective FEA models.

the response between the MMµGR-S and MMµGR-L sized versions may be attributed to variations in the magnets used. The MMµGR-S versions may have experienced inconsistencies in magnet properties due to oxidation of exposed 100 µm-sized NdFeB in the magnets. In contrast, the MMµGR-L type, equipped with the 250 µm-sized nickel-coated magnets, were less susceptible to such degradation due to their protective coatings.

C. Locomotion

By strategically aligning two magnets with slight variations in magnetic moment orientations, we create a net magnetic moment directed toward the front of the microrobot. This orientation control, enabled by external magnetic fields, allows us to precisely steer and orient the microrobot in a desired direction, as shown in Fig. 8. This level of independent control is particularly crucial in micromanipulation tasks, where precision and dexterity are paramount. At the microscale, traditional manipulation techniques become in-

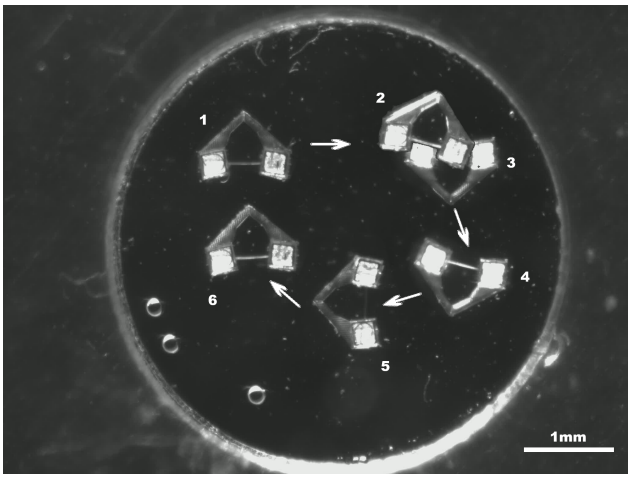

Fig. 8: Rotation and translation experiments: The NC MMμGR-L version is shown exhibiting its ability to independently rotate and translate. The MMμGR starts in position 1 and translates sideways to position 2. It then turns 180° and translates to position 4 where it rotates 90°. It then travels to position 5 and rotates 90° again to arrive at position 6.

creasingly challenging due to the limitations imposed by the physical size and the inherent forces at play. Magnetic field-based orientation and gradient control provide a non-invasive and highly precise means to manipulate microrobots with finesse. In this experiment, the MMμGR-L was manipulated to translate and reorient itself in a rectangular trajectory in the workspace. A 5mT magnetic field was used to control the orientation and gradients up to 1.5 T/m were utilized to induce translation.

D. Object Manipulation and Transport

To demonstrate the MMμGRs ability to capture and transport objects, we 3D printed 40 μm and 200 μm spheres in the same manner as we printed the microrobot body. These spheres were placed in the silicone oil with the MMμGR prototypes. Fig. 9 shows the MMμGR-L microrobots' ability to pick up 200 μm microbeads and arrange them into a triangular pattern. This showcases the microrobots' effectiveness in handling and accurately positioning microscale objects. Fig. 10 shows the MMμGR-S picking up and transporting a 40 μm cube to a desired location. The gripping mechanism, facilitated by the microrobots' compliant structures and magnetic field control, enables controlled manipulation of microscale objects through both pushing and pulling actions. These actions allow our microrobots to securely hold, transport, and position microbeads or other microscale components as needed. Our magnetic field-controlled microrobots exhibit impressive capabilities for manipulating and transporting microscale objects, with a specific focus on gripping, positioning, and precise arrangement. These functionalities are essential for applications in micro-assembly, lab-on-a-chip systems, and microscale patterning.

V. CONCLUSIONS

The field of microrobotics continues to push the boundaries of what is possible at the microscale. This paper

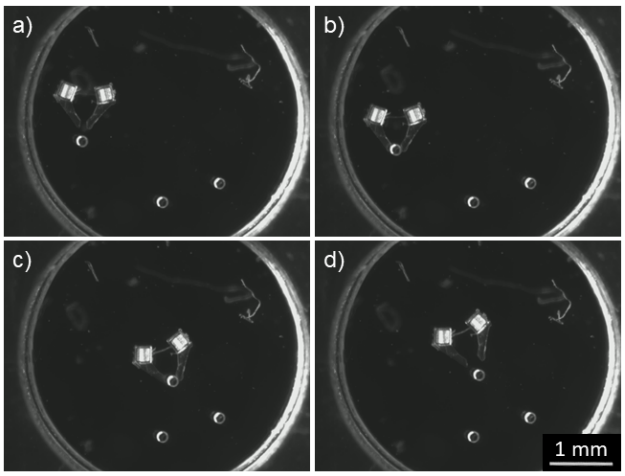

Fig. 9: MMμGR-L Micromanipulation experiments: The normally closed MMμGR-L version (a) translated to, (b) picking up, (c) transporting, and (d) dropping off the final bead in the assembly of a triangle pattern.

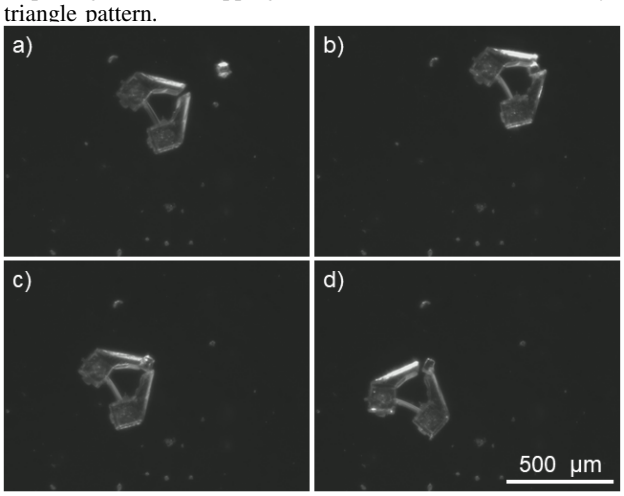

Fig. 10: MMμGR-S Micromanipulation experiments: The normally closed MMμGR-S version (a) translated to, (b) picking up, (c) transporting, and (d) dropping off a 40 μm cube

has explored the current state of microrobotics and micromanipulation, highlighting the pivotal role of magnetic field control in enabling precise and versatile microrobot behavior. By building upon the rich foundation laid by previous research, we have presented an innovative approach to magnetic field-controlled microrobots. Our work endeavors to bridge the gap between millimeter-scale and micrometer-scale microrobotics, introducing a novel design concept that utilized a two photon 3D printing and a novel assembly method to enable the creation of the smallest documented wireless magnetically actuated microgripper, as shown in Table II.

As we look to the future, the potential applications of magnetic field-controlled microrobots are vast, spanning fields such as microsurgery, microassembly, and microscale exploration. The insights gained from this research open new avenues for innovation, offering a platform for future advancements in microrobotics. By contributing to the growing body of knowledge in this field, we anticipate that our research will inspire further exploration and innovation.

TABLE II: Magnetically actuated mobile microgrippers by size

Style	Magnetization Method	Robot Size	Object size	Citation
Soft Hydrogel	Iron Oxide Nanoparticles	5.8 mm	2 mm	[10]
Hinged Box	Neodymium micorparticles	3.5 mm	400 µm	[9], [20], [21]
Tweezers	Neodymium microparticles	1-2 mm	250 µm	[11]
Tweezers (MMµGR-L)	Neodymium Cube	997 µm	200 µm	This Work
Tweezers (MMµGR-S)	Neodymium Cube	400 µm	40 µm	This Work

REFERENCES

[1] N. Ebrahimi, C. Bi, D. J. Cappelleri, *et al.*, "Magnetic actuation methods in bio/soft robotics," *Advanced Functional Materials*, vol. 31, no. 11, p. 2 005 137, 2021.

[2] G. Shao, H. O. T. Ware, J. Huang, R. Hai, L. Li, and C. Sun, "3d printed magnetically-actuating micro-gripper operates in air and water," *Additive Manufacturing*, vol. 38, Feb. 2021, ISSN: 22148604.

[3] H. Shen, S. Cai, Z. Wang, Z. Ge, and W. Yang, *Magnetically driven microrobots: Recent progress and future development*, Mar. 2023.

[4] D. Liu, T. Wang, and Y. Lu, "Untethered microrobots for active drug delivery: From rational design to clinical settings," *Advanced Healthcare Materials*, vol. 11, pp. 1–29, 3 2022, ISSN: 21922659.

[5] C. Yin, F. Wei, Z. Zhan, *et al.*, "Untethered microgripper-the dexterous hand at microscale," *Biomedical Microdevices*, vol. 21, 4 Dec. 2019, ISSN: 15728781.

[6] J. C. Kuo, H. W. Huang, S. W. Tung, and Y. J. Yang, "A hydrogel-based intravascular microgripper manipulated using magnetic fields," *Sensors and Actuators, A: Physical*, vol. 211, pp. 121–130, 2014, Hydrogel based microgripper using AC magnetic field heating based acuation., ISSN: 09244247.

[7] J. Cui, T. Y. Huang, Z. Luo, *et al.*, "Nanomagnetic encoding of shape-morphing micromachines," *Nature*, vol. 575, pp. 164–168, 7781 Nov. 2019, ISSN: 14764687.

[8] T. Xu, J. Zhang, M. Salehizadeh, O. Onaizah, and E. Diller, "Millimeter-scale flexible robots with programmable three-dimensional magnetization and motions," *Science Robotics*, vol. 4, 29 Apr. 2019, ISSN: 2470-9476.

[9] J. Zhang and E. Diller, "Tetherless mobile micrograsping using a magnetic elastic composite material," *Smart Materials and Structures*, vol. 25, 11 Oct. 2016, ISSN: 1361665X.

[10] S. R. Goudu, I. C. Yasa, X. Hu, H. Ceylan, W. Hu, and M. Sitti, "Biodegradable untethered magnetic hydrogel milli-grippers," *Advanced Functional Materials*, vol. 30, 50 2020, ISSN: 16163028.

[11] E. Diller and M. Sitti, "Three-dimensional programmable assembly by untethered magnetic robotic micro-grippers," *Advanced Functional Materials*, vol. 24, pp. 4397–4404, 28 Jul. 2014, ISSN: 16163028.

[12] B. Ahmad, A. Barbot, G. Ulliac, and A. Bolopion, "Ieee transactions on mechatronics remotely actuated optothermal robotic microjoints based on spiral bimaterial design."

[13] G. Stoychev, N. Puretskiy, and L. Ionov, "Self-folding all-polymer thermoresponsive microcapsules," *Soft Matter*, vol. 7, pp. 3277–3279, 7 2011, ISSN: 1744683X.

[14] D. Martella, S. Nocentini, D. Nuzhdin, C. Parmeggiani, and D. S. Wiersma, "Photonic microhand with autonomous action," *Advanced Materials*, vol. 29, 42 Nov. 2017, ISSN: 15214095.

[15] J. S. Randhawa, T. G. Leong, N. Bassik, B. R. Benson, M. T. Jochmans, and D. H. Gracias, "Pick-and-place using chemically actuated microgrippers," *Journal of the American Chemical Society*, vol. 130, pp. 17 238–17 239, 51 Dec. 2008, ISSN: 00027863.

[16] C. Peters, V. Costanza, S. Pane, B. J. Nelson, and C. Hierold, "Superparamagnetic hydrogels for two-photon polymerization and their application for the fabrication of swimming microrobots," *2015 Transducers - 2015 18th International Conference on Solid-State Sensors, Actuators and Microsystems, TRANSDUCERS 2015*, pp. 764–767, 2015.

[17] H. Ceylan, I. C. Yasa, O. Yasa, A. F. Tabak, J. Giltinan, and M. Sitti, "3d-printed biodegradable microswimmer for theranostic cargo delivery and release," *ACS Nano*, vol. 13, pp. 3353–3362, 3 2019, ISSN: 1936086X.

[18] S. Tottori, L. Zhang, F. Qiu, K. K. Krawczyk, A. Franco-Obregõn, and B. J. Nelson, "Magnetic helical micromachines: Fabrication, controlled swimming, and cargo transport," *Advanced Materials*, vol. 24, pp. 811–816, 6 2012, ISSN: 09359648.

[19] S. Lee, S. Kim, S. Kim, *et al.*, "A capsule-type microrobot with pick-and-drop motion for targeted drug and cell delivery," *Advanced Healthcare Materials*, vol. 7, pp. 1–6, 9 2018, ISSN: 21922659.

[20] J. Zhang, O. Onaizah, K. Middleton, L. You, and E. Diller, "Reliable grasping of three-dimensional untethered mobile magnetic microgripper for autonomous pick-and-place," *IEEE Robotics and Automation Letters*, vol. 2, pp. 835–840, 2 Apr. 2017, ISSN: 23773766.

[21] J. Zhang, M. Salehizadeh, and E. Diller, "Parallel pick and place using two independent untethered mobile magnetic microgrippers," IEEE, May 2018, pp. 123–128, ISBN: 978-1-5386-3081-5.